Photoelectron spectroscopy of $Si_2C_3^-$ and quantum chemistry of the linear Si_2C_3 cluster and its isomers

Xiaofeng Duan, Larry W. Burggraf, and David E. Weeks
Department of Engineering Physics, Air Force Institute of Technology, Wright-Patterson Air Force Base, Ohio 45433-7765

Gustavo E. Davico,[a] Rebecca L. Schwartz, and W. Carl Lineberger
JILA, University of Colorado and National Institute of Standards and Technology, and Department of Chemistry and Biochemistry, University of Colorado, Boulder, Colorado 80309-0440

(Received 6 June 2001; accepted 23 October 2001)

The 364 nm photoelectron spectrum of $Si_2C_3^-$ is reported, together with high level *ab initio* calculations of the linear anion, and six linear and eight nonlinear structures of the neutral Si_2C_3. The adiabatic electron affinity of Si_2C_3, corresponding to the transition from the linear anion to the lowest electronic state of the linear singlet neutral, is found to be 1.766 ± 0.012 eV. Theoretical results were essential for interpreting the spectrum. The level of theory necessary to accurately describe the electronic structure of Si_2C_3 cluster isomers is presented and discussed. Several vibration frequencies for the neutral linear structure are obtained from the spectra and compared to results from different levels of theory. © *2002 American Institute of Physics.*
[DOI: 10.1063/1.1427709]

I. INTRODUCTION

Intensive experimental and theoretical studies have been done on pure carbon and silicon clusters to understand chemistry in interstellar space as well as to look for their potential industrial applications.[1–17] Silicon-carbide clusters are potentially important to develop new materials such as electronic and electro-optic thin films made by chemical vapor deposition and pulsed laser deposition.[18] It is well known that the electronic properties of pure carbon and silicon clusters are quite different from each other and that properties of both types of clusters have strong dependence on their size and structure. However, the effect of stoichiometry on the structure and properties of mixed silicon carbide clusters is not well known. Understanding the variability of structure and spectroscopic properties silicon-carbon clusters with stoichiometry is important for applications of silicon-carbon clusters. Their structures and chemistry are also of fundamental interest to understand the nature of the chemical bonds in the clusters[12,19,20] and the effects of doping[21] and of substituting silicon atoms in the more stable carbon clusters.

This article reports the photoelectron spectrum of $Si_2C_3^-$ as well as the level of theory necessary to accurately describe the electronic structure of Si_2C_3 isomers. Although there have been many studies on pure carbon or silicon clusters,[22–28] fewer experimental and theoretical studies have been done for silicon carbide clusters. In the last few years, Si_2C_3 has been the subject of several experimental and theoretical investigations. Graham *et al.*[29] carried out Fourier transform infrared measurements of Si_2C_3 trapped in a solid argon matrix and, in conjunction with *ab initio* calculations by Rittby,[30] identified two fundamental vibrations: the C=C stretching mode $\nu_3(\sigma_u) = 1955.2\ \mathrm{cm}^{-1}$ and the Si–C stretching mode $\nu_4\ (\sigma_u) = 898.9\ \mathrm{cm}^{-1}$ of the centrosymmetric linear Si–C–C–C–Si configuration. Saykally *et al.*[31] characterized the $\nu_3(\sigma_u)$ band of linear Si_2C_3 by infrared spectroscopy. In addition, Nakajima *et al.*[32] carried out anion photoelectron spectroscopy on various cluster sizes of Si_mC_n, but due to low resolution, only vertical detachment energies were accurately reported. Theoretical studies have been done and have mainly focused on determination of structure and vibration spectra with either *ab initio* Hartree–Fock (HF)[30,33–35] or Density Functional Theory (DFT)[12,18,19] calculations.

Also, directly relevant to the photoelectron spectrum of $Si_2C_3^-$ is the C_5^- threshold photodetachment study reported by Kitsopoulos *et al.*[36] In their investigation, the authors showed that C_5^- is a linear molecule with a $^2\Pi_{1/2,3/2}$ ground state, with a 22 cm^{-1} spin-orbit splitting. They also show that the photodetachment threshold region contains substantial contributions from sequence bands of the lowest frequency skeletal bending mode, $\nu 7$. The frequency of this mode in the neutral is $\sim 100\ \mathrm{cm}^{-1}$, and about twice this value in the anion. They also find the $C_5 a\ ^3\Pi_g$ state lying ~ 0.25 eV above the $X\ ^1\Sigma_g$ ground state.

In this paper, details on Si_2C_3 are reported from photoelectron spectroscopy experiments. Motivated by the experimental observations, Si_2C_3 clusters were studied using HF, DFT, and Multi-Configuration Self-Consistent Field (MCSCF) calculations. The lower energy structures of the Si_2C_3 isomers for both singlet and triplet states were first determined. Then the electronic structure of the most stable centrosymmetric linear structure was calculated to accurately model the vibration spectra and electron affinity as compared to experimental results.

[a]Present address: Department of Chemistry, University of Idaho, Moscow, ID 83844-2343.

II. METHODS

A. Experiment

Si_mC_n anions are formed by using a cold cathode discharge. In this experiment, the cathode is a silicon carbide rod with a 5 mm diameter (Goodfellow Corporation). Clusters are sputtered from the cathode with a dc discharge in the presence of a mixture of 10–15% of argon in a helium buffer gas when Ar^+ is accelerated towards the negatively biased cathode.[37,38] The cathode voltage is approximately 2300 V with respect to grounded flow tube. The experiment can be performed at room temperature yielding a vibrational temperature of ~300 K or under liquid nitrogen cooled conditions that lower the vibrational temperature to ~180 K. Details of the negative ion photoelectron spectrometer used in this study have been published elsewhere.[39]

Multiple species of varying masses are made from the sputtering source. All anions are extracted and accelerated to 735 eV before being mass selected using a Wien filter. Currents of a few picoamperes of mass selected anions were produced during our experiments and were very dependent on the ion stoichiometry and flow tube temperature. The ion beam is decelerated to 40 eV prior to interacting with the 364 nm line from an argon ion laser. The electron-kinetic energy of the detached electrons is monitored with a hemispherical analyzer and a position sensitive detector, located perpendicular to the plane formed by the laser and ion beams. The effective resolution is 8 meV, and the absolute energy of narrow peaks in the spectrum can be determined to an accuracy of better than 5 meV via comparison with the established atomic oxygen photoelectron spectrum.[40] Spectra were collected at three different laser polarization angles (Θ) with respect to the direction of the collected electrons: 0°, 54.7°, and 90° (parallel, magic angle, and perpendicular).[41]

B. Computation

A variety of isomeric forms of Si_2C_3 clusters, six linear structures and eight nonlinear structures, were fully optimized using *ab initio* Hartree-Fock (HF) and DFT methods for both ground singlet (S_0) and triplet (T_0) electronic states. In DFT calculations Becke's three-parameter hybrid functional using the LYP correlation functional (B3LYP)[42–44] was employed. Dunning's correlation consistent double-zeta basis (cc-pVDZ) set[45] was used for both HF and DFT calculations. Vibration frequencies of all the species were computed at the same level of theory to verify that these structures were local minima or transition states.

Further calculations were made for the centrosymmetric Si–C–C–C–Si cluster, which has the lowest energy S_0 state among all the isomeric configurations. For the ground state neutral S_0 species and the anionic cluster in the ground doublet (D_0) state, the structures and vibration frequencies were optimized at B3LYP/cc-pVDZ level. The electron affinity (EA) was calculated by single point B3LYP calculations for neutral and anion cluster based on the structure optimized at B3LYP/cc-pVDZ, using basis sets aug-cc-pVTZ[46] and aug-cc-pV5Z,[47] which were augmented with the diffuse functions and triple and quintuple split for the valence shell.

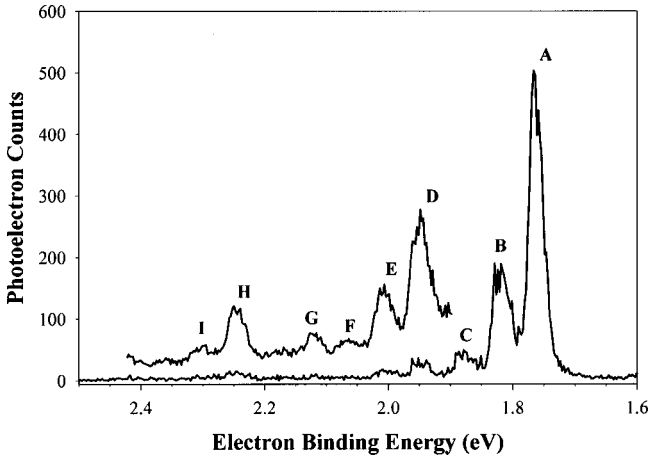

FIG. 1. The 364 nm photoelectron spectrum of $Si_2C_3^-$ taken at 180 K.

The zero-point energy corrections obtained at B3LYP/cc-pVDZ were accounted in the EA.

The DFT calculations were compared with HF, MP2 and MCSCF *ab initio* calculations, using the experimental electron affinity as a measure of the quality of the calculations. The structures and vibration frequencies of the neutral (closed and open shell) and anionic cluster at S_0, T_0, and D_0 states were also computed using these methods. For the MCSCF/cc-pVDZ calculations, both single and double excitation configuration interaction (CI) effects were considered in an active space of 20 valence electrons (21 for anion) in 20 orbitals. Next, Complete-Active-Space, [CAS (8-in-10)] MCSCF calculations were conducted with an active space made from eight π electrons distributed in ten π orbitals (four occupied and six virtual orbitals) with full CI in the space. Based on the optimized structures, some single point calculations with larger basis sets or higher levels of theory were carried out to obtain improved EA predictions. Specifically the CAS (8-in-10)/aug-cc-pVDZ and the second order Multi-Configuration Quasi-Degenerate Perturbation Theory (MCQDPT2) calculations that are based on CAS(8-in-10)/aug-cc-pVDZ reference wave functions were carried out. The calculations were carried out with GAUSSIAN 98[48] and GAMESS[49] computational chemistry packages.

III. RESULTS

A. Photoelectron spectra

The sputter ion source provided up to 10 pA of $Si_2C_3^-$, enabling collection of photoelectron spectra both at room temperature and with the flow tube cooled to 180 K. The 364 nm negative ion photoelectron spectrum of $Si_2C_3^-$ obtained with magic angle collection and with the flow tube cooled is shown in Fig. 1. The spectrum consists of nine identifiable transitions from the ground state of the anion to two different electronic states of the neutral. Peaks A–G arise from transitions from the anion ground state to the neutral singlet state of the linear $Si–C_3–Si$ isomer. The fact that virtually all of the vibration intensity is in peak A indicates that there is little change in the geometry of the cluster upon detachment of an electron from the anion, in agreement with theoretical calculations on the structures and geometries as discussed in Secs.

III B and III C. All of the peaks are broader than would be expected for a single vibronic transition subject to rotational broadening, and, indeed, peaks A–D show evidence of a doublet structure with comparable intensity in each component and a spacing between the doublets of about 8.5 meV, making them just barely resolvable with our apparatus. Further, temperature dependence studies show that at room temperature, the doublet structure is almost undetectable and the peak broadens asymmetrically to lower binding energy, indicative of the presence of hot bands. As discussed later this 60(30) cm^{-1} doublet corresponds to the spin-orbit splitting in the anion, and the broadening arises from sequence bands ($\Delta v = 0, \pm 2, ..$) involving the lowest frequency anion π-bending mode, $\nu 7$, analogous to the behavior observed by Kitsopoulos *et al.*[36] in C_5^-. The congestion is even worse, as a consequence of the substantial difference between the anion and neutral $\nu 7$ vibrational frequencies. Each of the peaks in the spectrum was fit to a Gaussian form; rotational peak shifts make a minor contribution to the overall uncertainty in the electron binding energy. The major uncertainties arise from the partially resolved vibration sequence bands and the spin-orbit coupling. The high binding energy component of the peak A doublet corresponds to the adiabatic EA of linear Si–C_3–Si, 1.766 ± 0.012 eV. The remaining peaks A-G (all doublets) could be fit with two active vibrations, with frequencies of $490 \pm 25\ cm^{-1}$ and $1520 \pm 25\ cm^{-1}$. The assignment of these frequencies to specific modes will be presented in the discussion.

Two weak peaks, H and I, appear too far above the origin (~0.5 eV) to be vibrational components of the $X\ ^1\Sigma_g$ ground state. While they might correspond to formation of an electronically excited state of the linear conformer, the very low intensity suggests that this is not the case. Peak H is the origin transition, with a binding energy of 2.245 ± 0.020 eV, and lies 0.480 ± 0.012 eV above the ground state. Peak I lies 420(25) cm^{-1} higher, and presumably corresponds to an active vibrational mode. Based upon all available evidence, we suggest that peaks H and I may arise from transitions involving the nonlinear structure, NL1, shown in Fig. 2. Details of all assignments are discussed in Sec. IV.

Photoelectron angular distributions were obtained in order to provide additional information on the origin of the features in the spectrum. The angular distributions of all transitions are essentially isotropic, giving an asymmetry parameter β value of zero.[41] This result is consistent with (but does not prove) the interpretation that the detached electron comes from a π orbital, similar to the photoelectron spectroscopy studies of other Si_mC_n anions.[50]

B. Structures of Si_2C_3 isomers

Six linear and eight nonlinear isomers of Si_2C_3 with relative energies ranging from 0–12 eV were optimized for both first singlet S_0 and triplet T_0 states (see Table I). The structures are shown in Fig. 2 and the geometric parameters and relative energies are listed in Tables II and III. It has been previously shown in both theoretical[19,30] and experimental[29,31,32] studies that the centrosymmetric linear structure Si–C–C–C–Si (L1) at $^1\Sigma_g^+$ is the ground state of

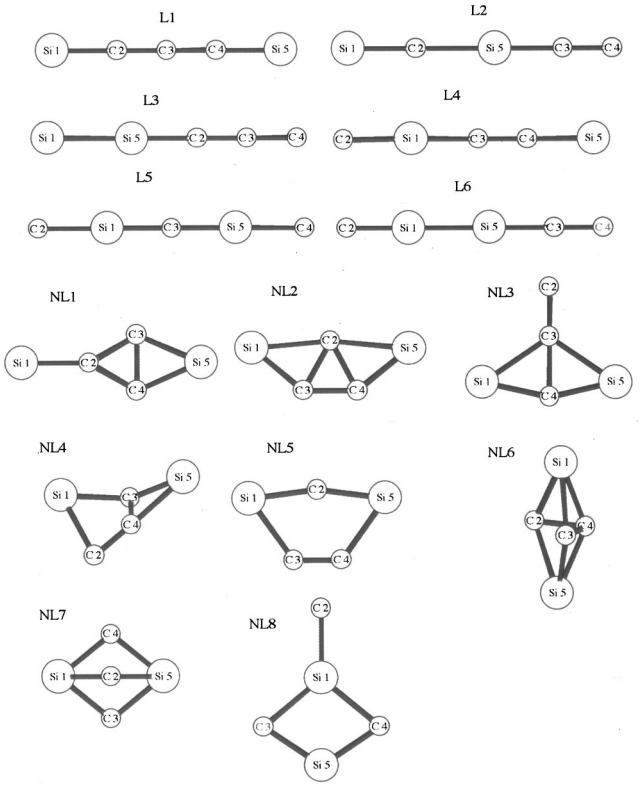

FIG. 2. Si_2C_3 isomer structures optimized using both HF/cc-pVDZ and B3LYP/cc-pVDZ levels of theory. Geometries and energies are given in Table I and Table II.

Si_2C_3. Our calculations using HF/cc-pVDZ and B3LYP/cc-pVDZ agree with this observation. Generally, HF/cc-pVDZ and B3LYP/cc-pVDZ calculations are consistent with each other for predictions of structures and their energy order, although in most cases the latter gives higher relative energies. Compared to the structure of L1 calculated by Rittby,[30] HF calculations with cc-pVDZ basis sets and DZP basis sets result in almost identical C–C and Si–C bond lengths. The B3LYP/cc-pVDZ structure is comparable to Rittby's MBPT(2)/DZP structure except for smaller bond distances (1.704 Å versus 1.720 Å for the Si–C bonds and 1.297 Å versus 1.308 Å for the C–C bonds), which are closer to coupled cluster predictions by Botschwina (1.686 Å and 1.289 Å).[19,30]

In Fig. 2, L1 to L6 include all possible linear structures that the Si_2C_3 cluster can have. The L1 linear structure has the lowest energy in as expected from the following two observations: (1) the greater strength of C–C bonds as compared to the Si–C or Si–Si bonds and (2) the stabilization of $-C_n-$ groups with double bonds such as $-C_3-$ subgroup in the middle of the Si_2C_3 carbon cluster. Reasoning from the explanation for L1, the higher energies of the other linear clusters, L2 to L6, can also be understood. In the L2 structure, the $-C_3-$ subgroup is broken and the energy therefore is increased to 2.1 eV at HF/cc-pVDZ level and 2.8 eV at B3LYP/cc-pVDZ level. In L3, not only does the $-C_3-$ subgroup no longer exist, but also the weak Si–Si bond further reduces the stability. In the L3 cluster, as well as in the rest of the linear clusters, the open-shell T_0 structure is more

TABLE I. Structural parameters and energetics of linear isomers of Si_2C_3 cluster.

		Bond Length Parameter, Å				Relative Energy, eV			
		HF		DFT		HF		DFT	
Isomer		S_0	T_0	S_0	T_0	S_0	T_0	S_0	T_0
L1	Sym.	$D_{\infty h}$	$D_{\infty h}$	$D_{\infty h}$	$D_{\infty h}$	0.000	1.586	0.000	1.530
	Si_1-C_2	1.672	1.739	1.704	1.763				
	C_2-C_3	1.287	1.282	1.297	1.296				
L2	Sym.	$C_{\infty h}$	$C_{\infty h}$	$C_{\infty h}$	$C_{\infty h}$	2.127	4.269	2.770	6.354
	Si_1-C_2	1.671	1.866	1.695	1.750				
	C_2-Si_5	1.649	1.670	1.675	2.024				
	Si_5-C_3	1.667	1.667	1.687	1.750				
	C_3-C_4	1.262	1.264	1.282	1.293				
L3	Sym.	$C_{\infty h}$	$C_{\infty h}$	$C_{\infty h}$	$C_{\infty h}$	4.230	3.446	4.614	4.016
	Si_1-Si_5	2.127	2.156	2.169	2.233				
	Si_5-C_2	1.717	1.760	1.718	1.725				
	C_2-C_3	1.278	1.248	1.294	1.291				
	C_3-Si_4	1.285	1.341	1.304	1.317				
L4	Sym.	$C_{\infty h}$	$C_{\infty h}$	$C_{\infty h}$	$C_{\infty h}$	5.920	4.534	4.757	5.108
	Si_1-C_2	1.702	1.719	1.745	1.772				
	Si_1-C_3	1.751	1.783	1.748	1.761				
	C_3-C_4	1.251	1.223	1.274	1.263				
	C_4-Si_5	1.714	1.847	1.740	1.793				
L5	Sym.	$D_{\infty h}$	$C_{\infty h}$	$D_{\infty h}$	$D_{\infty h}$	10.116	8.807	9.810	9.424
	Si_1-C_2	1.791	1.800	1.770	1.806				
	Si_1-C_3	1.660	1.658	1.700	1.698				
	C_3-Si_5		1.652						
	Si_5-C_4		1.823						
L6	Sym.	$C_{\infty h}$	$C_{\infty h}$	$C_{\infty h}$		12.635	7.224	6.815	
	Si_1-C_2	1.594	1.846	1.743					
	Si_1-Si_5	2.074	2.102	2.162					
	Si_5-C_3	1.679	1.672	1.689					
	C_3-C_4	1.267	1.269	1.290					

stable than the closed-shell S_0 structure; it has energy higher by 3.4 eV and 4.0 eV at HF and DFT levels, respectively. Following the same principle, the further decrease of instability from L4 to L6 can be readily rationalized. In order to check whether the structures are local minima or transition states, vibrational frequencies were calculated for each of the linear clusters. Except for L1, all the S_0 structures are transition states (L5 is a secondary transition state structure). Most T_0 structures are transition states (L2 is in the secondary transition state) and only L3 and L4 have local minimum structures.

Seven nonlinear Si_2C_3 isomers were previously optimized at the HF/6-31G(d) level.[30] In this work, the structures of these nonlinear isomers were recalculated at both HF/cc-pVDZ and B3LYP/cc-pVDZ levels of theory. The results, shown in Table II, are in good agreement with the previous work. In addition, a cyclic structure (NL5) was identified for which both S_0 and T_0 states have transition structures, as verified by vibration frequency calculations. Among the eight isomers, five of them have planar structures with C_{2v} symmetries. Among all the nonlinear isomers, NL7 has highest symmetry (D_{3h}) while NL4 has the lowest (C_1 at S_0 and C_s at T_0). For isomers from NL1 to NL5, S_0 states have lower relative energies by an amount in the range of 1.5 eV to 2.5 eV. For isomers from NL6 to NL8, T_0 states have lower energy and the relative energies increase rapidly from 3.5 eV to approximately 10.0 eV.

C. The centrosymmetric linear cluster

The geometry of the L1 cluster was fully optimized, without assumed symmetry, using different methods including HF, MCSCF, CAS, and B3LYP all with cc-pVDZ basis sets. The structure parameters found are listed in Table III. At HF level of theory, we obtained bond lengths of 1.672 Å for Si–C bonds and 1.287 Å for C–C bonds, which are nearly identical to Rittby's calculations[30] at the HF/DZP level of theory, but differ slightly from their HF/6-31G(d) results (1.66 Å and 1.28 Å). The DFT B3LYP, MCSCF(20,20) and CAS(8,10) optimizations results give similar bond lengths which are consistent with the MBPT(2)/DZP[30] structure (1.720 Å and 1.308 Å). Comparing these DFT and post-SCF geometries with the HF geometry, it is clear that calculations lacking electron correlation corrections underestimate both Si–C and C–C bond lengths in this silicon-carbide cluster.

The total electronic state has $^1\Sigma_g^+$ symmetry. The phase patterns of the valence shell molecular orbitals (occupied and virtual) obtained with HF methods are shown in Fig. 3. The

TABLE II. Structural parameters and energetics of nonlinear isomers of Si_2C_3 cluster.

		Bond length parameter (Å)				Relative energy (eV)[a]			
		HF		DFT		HF		DFT	
Isomer		S_0	T_0	S_0	T_0	S_0	T_0	S_0	T_0
NL1	Sym.	C_{2v}	C_{2v}	C_{2v}	C_{2v}	$^1A_1$	$^3A_2$	$^1A_1$	$^3A_2$
	Si_1-C_2	1.732	1.876	1.751	1.884	1.502	1.703	1.919	2.663
	C_2-C_3	1.431	1.403	1.444	1.419				
	C_3-C_4	1.436	1.467	1.453	1.495				
	C_3-Si_5	1.813	1.836	1.846	1.873				
NL2	Sym.	C_{2v}	C_{2v}	C_{2v}	C_{2v}	$^1A_1$	$^3B_2$	$^1A_1$	$^3B_2$
	Si_1-C_2	2.048	1.874	2.045	1.896	1.630	1.910	1.840	2.422
	Si_1-C_3	1.726	1.619	1.768	1.619				
	C_2-C_3	1.463	1.895	1.469	1.902				
	C_3-C_4	1.404	1.288	1.426	1.320				
NL3	Sym.	C_{2v}	C_{2v}	C_{2v}	C_{2v}	$^1A_1$	$^3B_2$	$^1A_1$	$^3B_2$
	Si_1-C_2	2.060	2.188	2.091	2.147	1.697	2.376	2.428	3.090
	Si_1-C_4	1.740	1.809	1.764	1.840				
	C_2-C_3	1.271	1.290	1.289	1.311				
	C_3-C_4	1.586	1.413	1.562	1.422				
NL4	Sym.	C_1	C_s	C_1		$^1A_1$	$^3A''$	$^1A_1$	
	Si_1-C_2	2.036	1.846	2.011		1.815	3.771	2.228	
	Si_1-C_3	1.805	1.829	1.845					
	Si_5-C_3	1.777	1.755	1.696					
	Si_5-C_4	1.921	1.946	1.915					
	C_2-C_4	1.284	1.242	1.307					
	C_3-C_4	1.741	1.903	1.696					
	Si_1-Si_5	3.261	3.470	3.289					
NL5	Sym.	C_{2v}	C_{2v}	C_{2v}	C_{2v}	$^1A_1$	$^3B_1$	$^1A_1$	$^3A_2$
	Si_1-C_2	1.779	1.823	1.800	1.823	2.040	5.119	2.546	4.798
	Si_1-C_3	1.997	1.884	2.019	1.900				
	C_3-C_4	1.240	1.242	1.263	1.267				
NL6	Sym.	C_{2v}	C_{2v}	C_{2v}	C_{2v}	$^1A_1$	$^3B_2$	$^1A_1$	$^3B_2$
	Si_1-C_2	2.025	1.927	2.058	1.969	4.228	3.506	4.373	3.766
	Si_1-C_4	1.861	2.159	1.916	2.164				
	C_2-C_3	2.111	1.905	2.158	2.005				
	C_2-C_4	1.447	1.428	1.438	1.436				
ML7	Sym.	D_{3h}	D_{3h}	D_{3h}	D_{3h}	$^1A_1'$	$^3A_1'$	$^1A_1'$	$^3A_1'$
	Si_1-C_2	1.849	1.986	1.875	1.965	8.029	6.497	6.169	5.447
	C_2-C_3	2.176	1.525	2.276	1.595				
NL8	Sym.	C_{2v}	C_{2v}	C_{2v}	C_{2v}	$^1A_1$	$^3B_2$	$^1A_1$	$^3B_1$
	Si_1-C_2	1.796	1.796	1.821	1.741	10.091	7.189	10.907	9.872
	Si_1-C_3	1.959	1.733	1.853	1.864				
	C_3-Si_5	1.803	1.848	1.790	1.804				
	Si_1-Si_5	2.266	3.001	2.443	2.788				

[a]Based on the ground-state energy of centrosymmetric linear Si–C–C–C–Si cluster.

molecular orbitals included in the active space calculations are indicated there. There are four occupied π orbitals (two bonding and two antibonding), all located on the C_3 subgroup. There is little π bonding between silicon and carbon atoms. The π-type p electrons on both of the silicon atoms form electron lone pairs in sp-type σ orbitals. Table IV lists the hybridization analysis, proposed by Raghavachari[51] and adopted by Gomei[52] for SiC_n clusters, applied to the ground-state geometry of the centrosymmetric structure. The analysis shows that silicon atoms tend to be sp hybridized, while C atoms are inclined towards sp^2 hybridization, consistent with our calculated molecular orbitals. The fact that a silicon

TABLE III. The bond lengths (Å) of the centrosymmetric linear Si_2C_3 molecule in several electronic states.

		HF[a]	B3LYP	MCSCF(20, 20)	CAS(8, 10)
S_0 state	Si_1-C_2	1.672	1.703	1.695	1.700
	C_2-C_3	1.287	1.297	1.304	1.295
T_0 state	Si_1-C_2	1.749	1.763	1.760	1.758
	C_2-C_3	1.284	1.296	1.301	1.294
D_0 state	Si_1-C_2	1.689	1.719	1.718	1.722
	C_2-C_3	1.295	1.304	1.310	1.302

[a]At D_0 state a nonsymmetric linear structure which has lower energy was also optimized with HF/cc-pVDZ method. The bond lengths are: $Si_1-C_2=1.760$ Å, $C_2-C_3=1.252$ Å, $C_3-C_4=1.341$ Å, $C_4-Si_5=1.652$ Å.

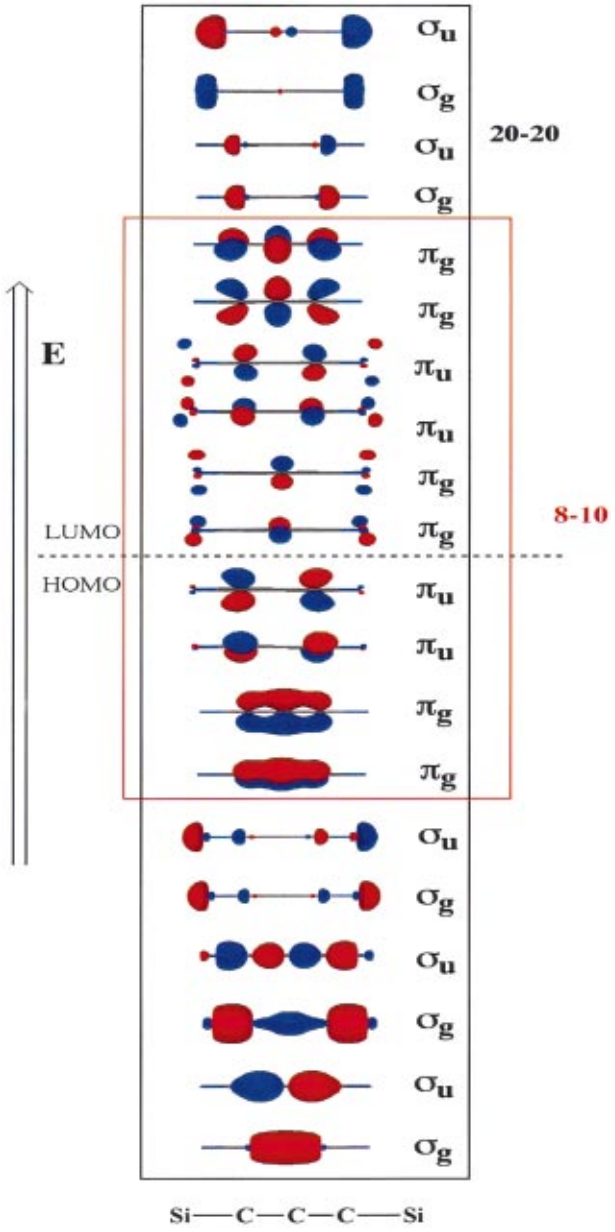

FIG. 3. (Color) Valence shell molecular orbital phase patterns (occupied and virtual) obtained with HF methods. Molecular orbitals included in (CAS) active space calculations are indicated.

terminated centrosymmetric linear cluster has lowest energy for Si_2C_3 clusters is consistent with the nature of silicon atoms to bond with less *sp* hybridization rather than making multiple bonds with carbon, as Gomei observed for SiC_n clusters.

There are seven normal vibrational modes in the ground state of Si_2C_3. Table V lists calculated and experimental harmonic vibration frequencies and their relative infrared intensities. Among these normal modes, $\nu 1$ and $\nu 2$ correspond to IR inactive symmetric stretching vibrations. The $\nu 3$ and $\nu 4$ modes are related to the antisymmetric stretching vibrations. Vibrational modes $\nu 5$, $\nu 6$ and $\nu 7$ are bending modes, where $\nu 5$ has *g* symmetry and is IR inactive. Computed vibration frequencies for the centrosymmetric anion are problematic because partially filled degenerate electron orbitals have

TABLE IV. Hybridization analysis for ground-state Mulliken charges at different states and extra electron distribution in the anionic cluster.

Method	Atom	Hybridization (S_0)	Mulliken charges S_0	T_0	D_0	Extra electron distribution
MCSCF	Si_1	$s2.01p1.99$	0.218	0.136	−0.261	−0.479
(20,20)	C_2	$s1.39p2.61$	−0.561	−0.486	−0.521	0.040
	C_3	$s1.57p2.43$	0.686	0.693	0.564	−0.122
B3LYP	Si_1		0.116	0.076	−0.369	−0.485
	C_2		−0.558	−0.516	−0.523	0.035
	C_3		0.882	0.881	0.782	−0.100
HF	Si_1		0.271	0.173	−0.243	−0.514
	C_2		−0.650	−0.521	−0.567	0.083
	C_3		0.758	0.697	0.620	−0.138

symmetries inconsistent with some vibration symmetries. In particular, computed bending modes in the *x-z* and *y-z* planes for the anion that should be degenerate are not. However, it is worthwhile to note that average estimates of $\nu 7$ for the anion [100(±7) and 107(±7) cm^{-1} by B3LYP/cc-pVDZ and CAS(8, 10)/cc-pVDZ, respectively] are similar to values for $\nu 7$ calculated for the neutral cluster.

We find, generally, that there is little difference in structure between the anion doublets and corresponding neutrals for small SiC clusters, a result consistent with their photoelectron spectra. For all computational methods, except for HF, the anionic cluster of C_3Si_2 retains a centrosymmetric linear geometry as shown in Table III. For the HF method both centrosymmetric and nonsymmetric D_0 C_3Si_2 structures were optimized. Although the nonsymmetric HF optimized structure is 0.19 eV lower in energy, it is believed the centrosymmetric isomer reflects the real structure as predicted by all correlation-correction methods.[53] Moreover, when both centrosymmetric and nonsymmetric structures are used to do MP2/cc-pVDZ single point calculations, the centrosymmetric structure gives a lower energy by 0.27 eV. Overall the structural changes from the linear neutral cluster to the anionic one are very small. For all of our calculations, forming the anion caused the Si–C and C–C bonds to increase by about 0.02 Å and 0.01 Å, respectively. As shown in the Table IV, in the anion the extra charge distributes its largest portion on silicon atoms and a smaller part on the middle carbon atom, while the carbons next to silicon atoms become slightly positive. This is consistent with the molecular orbital analysis, which shows that the electron goes to a π_g type LUMO of the neutral cluster and that occupation of *p* orbitals on silicon atoms increase. All three methods—MCSCF, B3LYP, and HF—predict the similar charge distribution patterns; however, the pattern from the HF calculation differs markedly from methods that include electron correlation corrections. For example, the positive charges on the C atoms next to the Si atoms calculated with HF are twice as large as those calculated with MCSCF and B3LYP. The map of the difference in total charge density between doublet and singlet electronic states shown in Fig. 4 further confirms that the B3LYP and MCSCF give comparable electron structures, while the HF method forecasts a significantly different electronic structure.

TABLE V. Vibration frequencies (cm^{-1}) and relative IR intensities of Si_2C_3 centrosymmetric linear cluster calculated at different levels of theory.

Method		$\nu_1(\sigma_g)$	$\nu_2(\sigma_g)$	$\nu_3(\sigma_u)$	$\nu_4(\sigma_u)$	$\nu_5(\pi_g)$	$\nu_6(\pi_u)$	$\nu_7(\pi_u)$
HF/cc-pVDZ	Frequencies	1712	509	2115	998	186	637	80
	Relative intensities	0.00	0.00	100.00	5.08	0.00	0.50	0.10
B3LYP/cc-pVDZ	Frequencies	1577	466	2052	904	206	580	84
	Relative intensities	0.00	0.00	100.00	9.05	0.00	0.67	0.14
CAS(8,10)/cc-pVDZ	Frequencies	1617	473	2105	929	220	568	108
	Relative intensities	0.00	0.00	100.00	5.29	0.00	0.82	0.10
MBPT(2)/DZP[a]	Frequencies	1527	442	2082	869	210	519	85
	Relative intensities	0.00	0.00	100.00	5.77	0.00	0.77	0.19
Experiment[b]	Frequencies			1955 (1968)[c]	899			
	Relative intensities			100.00	7.00			
Experiment[d]	Frequencies	1520±25	490±25					

[a]Rittby (Ref. 30).
[b]Ar matrix (Ref. 29).
[c]Gas phase (Ref. 31).
[d]This article.

The spin-orbit coupling between ground state and first excited state for the linear anion was estimated to be 57.5 cm^{-1}, using state-averaged CASSCF(3,5)/cc-pVDZ. Using CIS/cc-pVDZ calculations, the excitation energy from ground $^2\Pi$ state to first $^2\Sigma$ state is estimated to be 3.19 eV, much larger than the first π-π excitation energy of 0.69 eV.

IV. DISCUSSION

The primary peaks in photoelectron spectrum shown in Fig. 1 can be readily fit using a standard Franck–Condon modeling with two active vibrational modes. However, such a fit does not appropriately account for the breadth of the

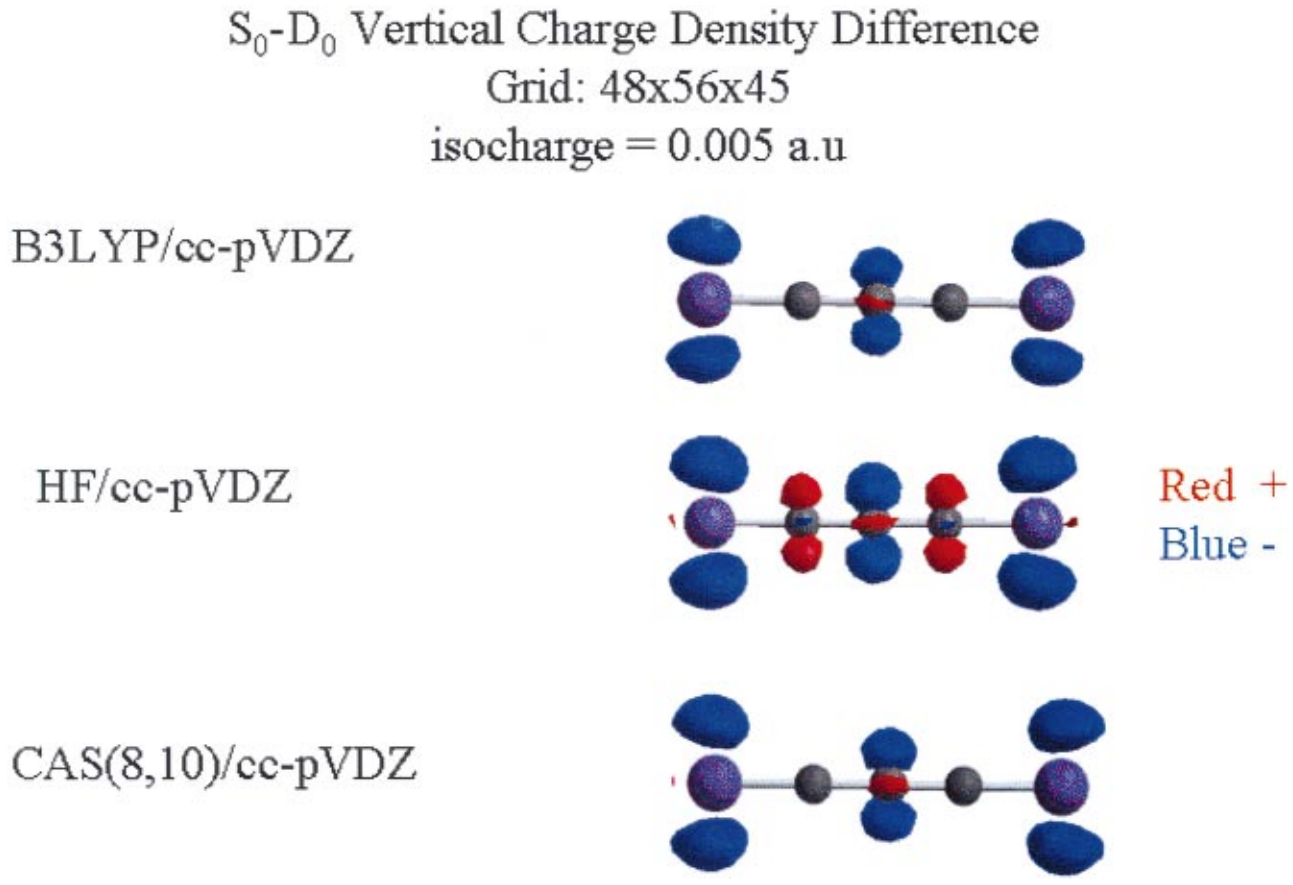

FIG. 4. (Color) Difference in total charge density between doublet and singlet electronic states for different levels of theory.

individual peaks, nor does it account for the observed temperature dependence of the peak shapes. It is possible to obtain a reasonable fit to the observations using several models:

(i) The anion might have a totally symmetric vibrational mode with a frequency of $\sim 100\ cm^{-1}$ and a large ($\sim 250\ cm^{-1}$) spin-orbit splitting.
(ii) The anion might have a low frequency non-totally symmetric vibrational mode (i.e., the π_u bends) with sufficiently different frequency in the neutral that the ($\Delta v = \text{even}$) photodetachment selection rule, together with sequence bands, produces the observed peak shape.
(iii) The anion spin-orbit splitting might be comparable to the observed peak width, with unresolved vibrations giving rise to the temperature-dependent broadening.

Each of these possibilities allows the choice of sets of parameters in the Franck-Condon fitting routine[39] that give a satisfactory fit to the observations. However, only model (iii) is consistent with all that is known about Si_2C_3 and $Si_2C_3^-$. Model (i) could fit the observations if an $\sim 80\ cm^{-1}$ totally symmetric vibration mode is assumed for the anion; the lowest frequency totally symmetric vibration mode is around $500\ cm^{-1}$, making this model untenable. Model (ii) presents more possibilities as the $\nu 7$ bending mode will be a low frequency, non-totally symmetric vibration mode in the anion, and the frequency of this mode should be much lower in the neutral. It is possible to fit the observations with an anion frequency of 100–200 cm^{-1}, *but* with the neutral $\nu 7$ being $80\ cm^{-1}$ lower. The C_5^- experiments of Kitsopoulos *et al.*[36] found just this circumstance, but with the anion $\nu 7$ frequency being $200\ cm^{-1}$, a frequency difference of $90\ cm^{-1}$. Given the larger mass of Si and the reluctance of Si to form π-bonds, both the $\nu 7$ frequency and the difference in SiC-CCSi is substantially less than in C_5. Thus, $\nu 7$ alone cannot produce the observed broadening.

Model (iii), however, provides a consistent interpretation. Each of the peaks A-G in the spectrum has the appearance of a doublet. While poorly resolved, the doublets can be fit with a splitting of 60(30) cm^{-1}. The uncertainty arises from the largely unknown and unresolved hot band components on each component. This splitting is completely consistent with the calculated $58\ cm^{-1}$ splitting reported here. This splitting must be present in the spectrum, and provides a constraint in the fit. However, all that can be concluded concerning the $\nu 7$ mode is that it has a relatively low frequency to provide the observed temperature effect. The final experimental parameters, then, are two vibrational frequencies, $490\ cm^{-1}$ and $1520\ cm^{-1}$, and an anion $^2\Pi$ spin-orbit splitting of 60(30) cm^{-1}.

The experimental spectrum with the simulation is displayed in Fig. 5. The vibrational frequencies are in good agreement with those calculated for the lowest σ_g modes, ν_2 and ν_1. These frequencies from B3LYP/cc-pVDZ and CAS(8,10)/cc-pVDZ are 466 and 1577 cm^{-1}, and 473 and 1617 cm^{-1}, respectively (Table V). Hartree–Fock level calculations yield higher frequencies for most of the bands, but if they are conventionally scaled (e.g., with a 0.8929 scaling factor for HF/6-31G(d) frequencies), frequencies close to experimental values are obtained. Similarly, both the experimental and theoretical frequencies presented here agree well with previous MBPT(2)/DZP[30] calculations and experimental observations.[29,31] Non-Franck–Condon modes in linear species were observed in previous experiments,[36,54] including smaller size silicon carbide clusters[50] and in the analogous case of C_5^-, for which such vibrations constituted[36] a major component of the spectrum.

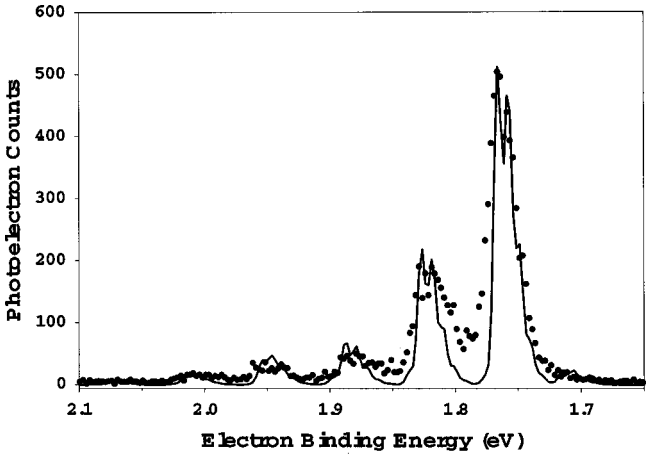

FIG. 5. The ground-state portion of the $Si_2C_3^-$ photoelectron spectrum (dots) and a Franck–Condon simulation of the spectrum using calculated anion and neutral structures (solid line). The simulation assumes a 60 cm^{-1} spin-orbit splitting in the anion, and 490 and 1520 cm^{-1} active vibrational modes in the neutral.

Vibration frequencies calculated by both B3LYP/cc-pVDZ and CAS(8,10)/cc-pVDZ, which are not observed in the photoelectron spectrum, also are in good agreement with previous work.[29,31] For the two most intense vibration bands, $\nu 3$ and $\nu 4$, B3LYP calculation gives closest values to the experimental results (Table V). Normal mode analysis indicates that the $\nu 3$ mode, which dominates the infrared (IR) spectrum, is mainly the antisymmetric C–C stretching of C_3 subgroup involving little displacements for silicon atoms. The $\nu 4$ band comes from the Si–C antisymmetric stretching mode and its absorption is related to the $\nu 3$ band as experimentally observed.[29] The calculated IR intensity ratio for $\nu 4/\nu 3$ at B3LYP level is 0.09, which compares well with the experimental IR value of 0.07. Similar to the B3LYP calculation, CAS(8,10) computed frequencies and relative intensities are also in good agreement with experimental values.

The electron affinity is the experimental parameter for silicon carbide clusters that is most difficult to accurately predict theoretically. The binding energy of Peak A in the experimental spectrum indicates that the adiabatic electron affinity of linear Si_2C_3 is $1.766 \pm 0.012\ eV$, significantly more accurate than the $1.5 \pm 0.1\ eV$ reported by Nakajima *et al.*[32] In calculations reported here, the electron affinity is determined as the energy difference between the energies of the neutral cluster and the anionic cluster, including zero-point energy corrections obtained from the calculated harmonic vibrational frequencies. To systematically search for the most suitable method for predicting EA for these clusters,

TABLE VI. The relative energies and electronic affinity of the Si_2C_3 centrosymmetric linear cluster calculated at different levels of theory. All energies are in units of eV.

Calculations	S_0	T_0	D_0	EA[a]
HF/cc-pVDZ	0.000	1.586	−0.675	0.637
			(−0.868)[b]	(0.901)[b]
MP2/cc-pVDZ//	0.000	1.738	−1.372	1.334
HF/cc-pVDZ			(−1.102)[b]	(1.135)[b]
B3LYP/cc-pVDZ	0.000	1.530	−1.474	1.512
B3LYP/aug-cc-pVTZ// B3LYP/cc-pVDZ	0.000	1.865	−1.651	1.689
B3LYP/aug-cc-pV5Z// B3LYP/cc-pVDZ	0.000		−1.704	1.742
MCSCF(20,20)/cc-pVDZ	0.000	1.395	−0.553	0.594
CAS(8,10)/cc-pVDZ	0.000	1.676	−0.743	0.784
CAS(8,10)/aug-cc-pVDZ	0.000		−0.896	0.937
MCQDPT2(8,10)/Aug-cc-pVDZ// CAS(8,10)/cc-pVDZ	0.000		−1.885	1.926
Experiment[c]				1.766

[a]$EA = \Delta E(S_0 - D_0) + \Delta ZPE(S_0 - D_0)$.
[b]Non-symmetric D_0 structure was used.
[c]This article.

we evaluated effects of the level of theory and also the size of the basis sets. Comparisons of calculated and experimental EA are listed in the last column of Table VI. The fact that the EA calculated using the HF/cc-pVDZ centrosymmetric structure lies 0.637 eV below the experimental value of 1.766 eV indicates that electron correlation plays a critical role in the determination of EA's of silicon-carbide clusters. The single point MP2/cc-pVDZ calculations largely accounted for electron correlation, and the calculated EA increased significantly, to 1.334 eV. It is known that the electron correlation correction is surprisingly well compensated by the B3LYP parameterization and this conclusion is further supported by our EA calculations. The EA calculated by B3LYP/ccp-pVDZ is 1.512 eV, in even better agreement with the experimental value. Enlarging the basis sets by augmenting with diffuse functions and increasing the splitting of the valence shell further improves the EA, as demonstrated by single point B3LYP calculations with aug-cc-pVTZ and aug-cc-pV5Z basis sets. It is impressive to observe that the B3LYP/aug-cc-pV5Z single point calculation gives an EA of 1.742 eV, only 1.5% below the experimental result.

When multiconfiguration CI methods like MCSCF(20,20) and CAS(8,10) were used, the calculated EA values fall in approximately the same range as HF calculations, as shown in Table VI. Augmenting the cc-pVDZ basis sets with a diffuse function improves the EA value somewhat, but it is still about 47% less than the experimental EA. This result can be understood by differences in reproducing static and dynamic correlation. Static correlation is primarily corrected in multiconfiguration CI methods, but the dynamic correlation, which has important effects on EA calculations, is not appropriately reproduced. Dynamic correlation can be adequately corrected by applying multistate and multireference perturbation theory, such as the MCQDPT2 method. Table VI shows that the single point MCQDPT2(8,10)/aug-cc-pVDZ calculations bring post-HF EA value up from 0.937 eV for CAS(8,10)/aug-cc-pVDZ calculations to 1.926 eV, which is only 9% higher than the experimental value. Gomei *et al.*[52] calculated EA's of SiC_m $(m=2-5)$ clusters with MP4/6-31G(d) and CCSD(T)/aug-cc-pVDZ methods. While their calculations were in agreement with the earlier[32] experimental observations, the error of their calculations was greater than ± 0.11 eV.

The structure parameters in Table III show that ROHF, B3LYP, MCSCF(20, 20) and CAS(8,10) calculations all predict a similar centrosymmetric linear geometry as the ground S_0 state. For the T_0 state, DFT and post SCF methods predict longer bond lengths for Si–C and C–C bonds than does the HF method. In T_0, the Si–C bonds stretch about 0.06 Å while the C–C bond does not change, with respect to the values for the S_0 state. Table VI shows the relative energies of different electronic states calculated for the cluster. The cluster at the T_0 state has a calculated energy about 0.9–1.9 eV higher than energy of the S_0 state depending on the calculation methods. The HF method gives lowest T_0 energy while the CAS(8,10) calculation produces the highest one. The methods that compensate for correlation (B3LYP, MCSCF(20,20), and CAS(8,10)) result in T_0 energies ranging from 1.4 eV to 1.9 eV. Increasing the quality of the basis set seems to increase the singlet-triplet gap. The splitting value obtained at B3LYP/aug-cc-pVTZ//B3LYP/cc-pVDZ level is about 0.3 eV higher than the same value obtained at the B3LYP/cc-pVDZ/B3LYP/cc-pVDZ level.

These results suggest that the second vibrational progression of peaks (peaks H and I) observed in the experimental spectrum, which appear 0.480 (0.003) eV above the ground state origin, do *not* arise from the triplet state of the L1 isomer. In addition, photodetachment of $SiCCCSi^-$ producing the lowest triplet state should have a cross section comparable to that for producing the ground state molecule. We observe a cross section some 30 times smaller, with no indication that the Franck–Condon overlap is particularly poor. Furthermore, we can rule out the possibility that this band originates from contaminating anions of similar mass, like CSi_3^- or C_5Si^-, that could not be completely resolved by our Wien filter (resolution ≈40), since photodetachment of these species does not produce photoelectrons in this range of binding energies.[50,55] Based upon this logic, a plausible assignment of peaks H and I is to transitions between the T_0 state of Si_2C_3 and the D_0 state of $Si_2C_3^-$ having the NL1 geometry shown in Fig. 2. The assignment is bolstered by noting that the EA of singlet NL1 is approximately 1.43 eV as determined by DFT calculations at the B3LYP/cc-pVDZ level. This level of calculation is observed to systematically underestimate the EA of SiC clusters by approximately 0.1 to 0.2 eV compared to higher level DFT calculations. The T_0 energy of NL1 is 0.744 eV above the S_0 energy as obtained from Table II, and when added to the EA of singlet NL1, yields a triplet NL1 EA of 2.18 eV. We therefore attribute the H peak at 2.245 eV to the ground vibrational state of triplet NL1. Vibration frequency analysis of triplet NL1 using unrestricted B3LYP/cc-pVDZ yields a symmetric mode at 400 cm^{-1} that we attribute to peak I, in close agreement with experiment. If a second isomer is present in the ion beam giving rise to peaks H and I, then it might well be expected that the intensity of these peaks rela-

tive to peaks A–G might change as ion source conditions are varied. That is indeed observed. However, the estimated binding energy of singlet NL1 would give a weak feature that could easily be buried underneath the intense peaks A and B. Thus, we lack this ability to confirm this assignment, and can only present it as a plausible possibility. Finally, we note that the H and I peaks also appear to be present in Nakajima's lower resolution spectrum.[32]

V. CONCLUSIONS

The 364 nm photoelectron spectrum of $Si_2C_3^-$ has been recorded and consists of nine features attributed to two different states. From the spectrum, an accurate value of the adiabatic electron affinity for the linear centrosymmetric isomer is determined to be 1.766 (0.012) eV. A progression of peaks (A–G) is observed and corresponds to various vibration states within the singlet state of the linear $Si-C_3-Si$ isomer. A simulation of the experimental spectrum is presented from which vibration frequencies have been obtained. These frequencies agree well with those determined theoretically. A second progression of peaks (H, I) at higher electron binding energies may arise from transitions to the triplet state of the nonlinear NL1 structure.

Six linear structures and eight nonlinear structures of Si_2C_3 were characterized in this work using HF/cc-pVDZ and DFT/cc-pVDZ methods. The experimental observation and theoretical calculation indicate that the centrosymmetric linear Si_2C_3 cluster is the most stable structure. Detailed investigation of the electronic structures of the centrosymmetric linear Si_2C_3 cluster at different levels of theory reveal that in the ground state with $^1\Sigma_g^+$ symmetry, there is little π bonding between silicon and carbon atoms. Hybridization analysis indicates that the silicon atoms tend towards *sp* hybridization while carbon atoms are inclined towards sp^2 hybridization. This observation is consistent with the fact that the Si-terminated linear clusters have lower energies. An analysis of the Si_2C_3 anion reveals very small geometry changes when compared to the neutral Si_2C_3 cluster, in agreement with experiments. A Mulliken charge analysis shows that the largest portion of the extra charge on the anion is distributed largely on the silicon atoms while a smaller portion is distributed on the middle carbon atom. The carbon atoms bonded to the silicon atoms become slightly positive.

The EA of the centrosymmetric linear Si_2C_3 cluster was calculated using several levels of theory and the results were compared with experimental observations. It was found that the electron correlation corrections, particularly dynamic correlation corrections, are crucial in determining the EA for silicon-carbide clusters. Neither HF nor MCSCF methods are able to address dynamical correlation, while MP2 and especially B3LYP methods compensate for correlation influences fairly well. Our best calculation using B3LYP/cc-pV5Z//B3LYP/cc-pVDZ gives an EA of 1.742 eV for which the error is only 1.5% compared to the observed value. The calculated ground state IR spectra of the Si_2C_3 cluster are in good agreement with experimental observations independent of the computational method used. For the most important $\nu 3$ and $\nu 4$ vibration bands, B3LYP/cc-pVDZ gives best peak positions and intensity ratio compared to the experimental values.

ACKNOWLEDGMENTS

The authors gratefully acknowledge AFOSR for funding this research and Dr. Mark Gordon of Iowa State University for helpful discussions. The views expressed in this article are those of the authors and do not reflect the official policy or position of the United States Air Force, Department of Defense, or the U.S. Government.

[1] W. J. Weltner and R. J. Van Zee, Chem. Rev. **89**, 1713 (1989).
[2] J. M. L. Martin, J. P. Francois, and R. Gijbels, J. Mol. Struct. **294**, 21 (1993).
[3] S. Sugano, *Microcluster Physics* (Springer Verlag, Germany, 1991).
[4] K. Raghavachari and J. S. Binkley, J. Chem. Phys. **87**, 2191 (1987).
[5] J. M. L. Martin, J. P. Francois, and R. J. Gijbels, J. Chem. Phys. **59**, 8850 (1990).
[6] J. Koutecky and P. Fantucci, Chem. Rev. **86**, 539 (1986).
[7] H. W. Kroto, J. R. Heath, S. C. O'Brien, R. F. Curl, and R. E. Smalley, Nature (London) **318**, 162 (1985).
[8] P. W. Fowler and D. E. Manolopoulos, *An Atlas of Fullerenes and their Derivatives* (Oxford University Press, New York, 1995).
[9] J. P. Lu and W. Yang, Phys. Rev. B **49**, 11421 (1994).
[10] E. Kaxiras and K. Jackson, Phys. Rev. Lett. **71**, 727 (1993).
[11] U. Rothlisberger, W. Andreoni, and M. Parrinello, Phys. Rev. Lett. **72**, 665 (1994).
[12] M. Bertolus, V. Brenner, and P. Millie, Eur. Phys. J. D **1**, 197 (1998).
[13] L. A. Curtiss, P. W. Deutsch, and K. Raghavachari, J. Chem. Phys. **96**, 6868 (1992).
[14] C. M. Rohlfing and K. Raghavachari, Abstr. Pap. - Am. Chem. Soc. **202**, 79 (1991).
[15] K. Raghavachari and C. M. Rohlfing, Chem. Phys. Lett. **143**, 428 (1988).
[16] K. Raghavachari, Z. Phys. D: At., Mol. Clusters **12**, 61 (1989).
[17] K. Raghavachari and C. M. Rohlfing, J. Chem. Phys. **94**, 3670 (1991).
[18] J. D. Parsons, R. F. Bunshah, and O. M. Stafsudd, Solid State Technol. **28**, 133 (1985).
[19] S. Hunsicker and R. O. Jones, J. Chem. Phys. **105**, 5048 (1996).
[20] R. Juvencio and O. Mayorga, Nanostruct. Mater. **10**, 1317 (1998).
[21] K. Jug, M. Krack, and H. Nolte, Chem. Phys. Lett. **184**, 209 (1991).
[22] A. Van Orden and R. J. Saykally, Chem. Rev. **98**, 2313 (1998).
[23] D. W. Arnold, S. E. Bradforth, T. N. Kitsopoulos, and D. M. Neumark, J. Chem. Phys. **95**, 8753 (1991).
[24] C. Xu, G. R. Burton, T. R. Taylor, and D. M. Neumark, J. Chem. Phys. **107**, 3428 (1997).
[25] C. S. Xu, T. R. Taylor, G. R. Burton, and D. M. Neumark, J. Chem. Phys. **108**, 1395 (1998).
[26] T. N. Kitsopoulos, C. J. Chick, A. Weaver, and D. M. Neumark, J. Chem. Phys. **93**, 6108 (1990).
[27] T. N. Kitsopoulos, C. J. Chick, Y. Zhao, and D. M. Neumark, J. Chem. Phys. **95**, 1441 (1991).
[28] M. Kohno, S. Suzuki, H. Shiromaru, and Y. Achiba, J. Chem. Phys. **110**, 3781 (1999).
[29] J. D. Presilla-Marquez and W. R. M. Graham, J. Chem. Phys. **100**, 181 (1994).
[30] C. M. L. Rittby, J. Chem. Phys. **100**, 175 (1994).
[31] A. Orden, T. F. Van Giesen, R. A. Provencal, H. J. Hwang, and R. J. Saykally, J. Chem. Phys. **101**, 10237 (1994).
[32] A. Nakajima, T. Taguwa, K. Nakao, M. Gomei, R. Kishi, S. Iwata, and K. Kaya, J. Chem. Phys. **103**, 2050 (1995).
[33] P. W. Deutsch and L. A. Curtiss, Chem. Phys. Lett. **226**, 387 (1994).
[34] R. S. Grev and H. F. Schaefer, J. Chem. Phys. **82**, 4126 (1985).
[35] I. L. Alberts, R. S. Grev, and H. F. Schaefer III, J. Chem. Phys. **93**, 5046 (1990).
[36] T. N. Kitsopoulos, C. J. Chick, Y. Zhao, and D. M. Neumark, J. Chem. Phys. **95**, 5479 (1991).
[37] J. Ho, Ph.D. thesis, University of Colorado, 1991.
[38] J. Ho, K. M. Ervin, and W. C. Lineberger, J. Chem. Phys. **93**, 6987 (1990).
[39] K. M. Ervin and W. C. Lineberger, in *Advances in Gas Phase Ion Chemistry*, Vol. 1, edited by L. M. Babcock (JAI, Greenwich, CT, 1992), p. 121.

[40] D. M. Neumark, K. R. Lykke, T. Andersen, and W. C. Lineberger, Phys. Rev. A **32**, 1890 (1985).
[41] J. Cooper and R. N. Zare, J. Chem. Phys. **48**, 942 (1968).
[42] A. D. Becke, J. Chem. Phys. **98**, 5648 (1993).
[43] C. Lee, W. Yang, and R. G. Parr, Phys. Rev. B **37**, 785 (1988).
[44] B. Miehlich, A. Savin, H. Stoll, and H. Preuss, Chem. Phys. Lett. **157**, 200 (1989).
[45] D. E. Woon and T. H. Dunning, Jr., J. Chem. Phys. **98**, 1358 (1993).
[46] R. A. Kendall, T. H. Dunning, Jr., and R. J. Harrison, J. Chem. Phys. **96**, 6796 (1992).
[47] K. A. Peterson, D. E. Woon, and T. H. Dunning, Jr., J. Chem. Phys. **100**, 7410 (1994).
[48] M. J. Frisch, G. W. Trucks, H. B. Schlegel *et al.*, GAUSSIAN 98 Revision A.7, Gaussian, Inc., Pittsburgh, PA, 1998.
[49] M. W. Schmidt, K. K. Baldridge, J. A. Boatz *et al.*, J. Comput. Chem. **14**, 1347 (1993).
[50] G. E. Davico, R. L. Schwartz, and W. C. Lineberger, J. Chem. Phys. (in press).
[51] K. Raghavachari and C. M. Rohlfing, J. Chem. Phys. **89**, 2219 (1988).
[52] M. Gomei, R. Kishi, A. Nakajima, S. Iwata, and K. Kaya, J. Chem. Phys. **107**, 10051 (1997).
[53] X. F. Duan and D. S. Dudis (unpublished).
[54] K. M. Ervin and W. C. Lineberger, J. Phys. Chem. **95**, 1167 (1991).
[55] G. E. Davico, R. L. Schwartz, and W. C. Lineberger (unpublished).